Journal of Archaeological Science: Reports 71 (2026) 105679

Contents lists available at ScienceDirect

Journal of Archaeological Science: Reports

journal homepage: www.elsevier.com/locate/jasrep

Characterization and provenance studies of the stone *tesserae* from the "*A Grandi Fiori*" mosaic in the Roman villa of Casignana (Reggio Calabria, Italy)

Maria Antonietta Zicarelli [a,*], Luciana Randazzo [b,c], Natalia Rovella [a,d,*], Donatella Barca [a], Mauro Francesco La Russa [a], Michela Ricca [a]

[a] *Department of Biology, Ecology and Earth Sciences (DiBEST). University of Calabria, 87036 Arcavacata di Rende (CS), Italy*
[b] *Department of Earth and Marine Sciences (DiSTeM). University of Palermo 90123 Palermo (PA), Italy*
[c] *Istituto Nazionale di Geofisica e Vulcanologia (INGV) - Sezione di Palermo 90146 Palermo (PA), Italy*
[d] *Institute on Membrane Technology (CNR-ITM), Via P. Bucci 17/c, 87036 Rende, CS, Italy*

ARTICLE INFO

Keywords:
Archaeometry
Characterization
Mosaic
Provenance
Stone
White marbles

ABSTRACT

This study focuses on the archaeometric analysis carried out on the stone *tesserae* constituting the "*A Grandi Fiori*" Mosaic in "Room N" of the residential area of the Roman Villa at Palazzi di Casignana (Reggio Calabria, Italy). The mosaic, dated to the 3rd century CE, features green and white *tesserae* arranged in four-petaled floral motifs.

A multi-analytical approach was adopted to characterize both the green and white stone *tesserae* constituting the mosaic. In addition, provenance studies were conducted on the white marble *tesserae*. Data obtained from mineralogical and petrographic analyses using Polarized Optical Microscopy (POM), X-Ray Diffraction (XRD), and Scanning Electron Microscopy coupled with Energy Dispersive Spectroscopy (SEM-EDS) were combined. Furthermore, the determination of oxygen and carbon stable isotope compositions ($\delta^{13}C$ and $\delta^{18}O$) through mass spectrometry (MS) was performed on the white marble *tesserae*. The results from these investigations were compared with the recently updated reference databases of major Mediterranean marbles used in antiquity in order to evaluate their most probable origin.

The minero-petrographic investigation revealed the use of a biomicrite for the green tesserae. On the other hand, the petrographic and geochemical analyses of the white *tesserae* indicate the presence of marbles sourced from various regions, including Asia Minor, Greece, and Italy, with a predominant use of Proconnesian marble. The presence of mosaic *tesserae* sourced from distant Mediterranean areas further underscores the historical significance of the villa and provides new insights into the trade routes of raw materials in ancient Rome. At the same time, the evidence may suggest a possible reuse of marble leftovers, potentially related to the documented phases of structural transformation and renovation of the villa.

1. Introduction

The evolution of mosaic technique over time involved the use of a wide range of lithic materials, both natural and artificial, carefully shaped into *tesserae* and assembled according to well-defined decorative schemes.

Although traditionally interpreted in close relation to painting – often diminishing its autonomy as an artistic medium – the execution of mosaics required specialized workshops, skilled craftsmanship and a more complex level of technical preparation than that involved in pictorial techniques (Stern, 1975). Despite their artistic and historical significance, most studies on mosaics have focused primarily on the stylistic classification and art-historical analysis, while the technological aspects of production, and particularly the characterization of raw materials, have been less frequently investigated. Yet, the study of ancient mosaics can provide essential insights into the technological, economic, and cultural contexts of the ancient world. In fact, beyond their decorative role, mosaics represent valuable indicators of technical know-how, aesthetic preferences, and the social status of the *dominus* who commissioned them.

* Corresponding authors..
E-mail addresses: mariaantonietta.zicarelli@unical.it (M.A. Zicarelli), n.rovella@itm.cnr.it (N. Rovella).

https://doi.org/10.1016/j.jasrep.2026.105679
Received 22 December 2025; Received in revised form 12 February 2026; Accepted 3 March 2026
Available online 10 March 2026

In this framework, a multidisciplinary archaeometric approach, based on petrographic and geochemical analyses, represents an indispensable tool for tracing the provenance of stone materials, clarifying procurement strategies and identifying the cultural and economic choices underlying material selection.

Provenance studies have shown that raw materials were not exclusively sourced locally, where availability was easier, but often involved importing prestigious marbles and ornamental stones from distant provinces of the Empire. This practice reflects the high social status of the owners (Taelman, 2022). In certain cases, the presence of imported lithotypes may even suggest the mobility of professional workers and the diffusion of artistic techniques across the Roman world. Furthermore, archaeometric research can shed light on the motivation behind the choice of specific lithologies, determining whether such decisions were conditioned not only by the availability of stone resources but also by the evolution of mosaic styles (Flügel and Flügel, 1997). However, this framework should also take into account the widespread practice of material reuse in the Roman world. Substantial archaeological evidence indicates that a wide range of construction materials including wall facings, paving elements, sculpted architectural components, metal fittings and clamps, window glass, and roof tiles, were regularly salvaged, reworked, and reintroduced into new building phases or renovations, either through recutting, remodelling, or reprocessing (Munro, 2011).

In this context, the present research focuses on the archaeometric characterization of the stone *tesserae* from the *"A Grandi Fiori"* mosaic in "Room N" of the Residential Area of the Roman Villa at Palazzi di Casignana (Reggio Calabria, Italy) (Fig. 1a, b, c, d).

Extending over approximately 15 ha, the Villa of Casignana is one of the most monumental examples of Late Imperial architecture in southern Italy. It is richly decorated with elaborate floor mosaics and marble wall slabs, making it comparable to other major Late Antique complexes such as the Villa del Casale at Piazza Armerina in Sicily (Bruni, 2009).

This study aims to enhance current knowledge by conducting archaeometric analysis of mosaics from the Calabrian region. The findings will offer valuable insights into the dynamics of raw material exploitation and support the development of effective conservation and preservation strategies for this unique cultural heritage (Rovella et al., 2022; Ricca et al., 2020; Barca et al., 2019).

2. The archaeological site and the "*A Grandi Fiori*" mosaic

The Roman Villa of Casignana, located along the modern Strada Statale (SS) 106 between the towns of Bianco and Bovalino (Reggio Calabria), is one of the most significant archaeological sites in Calabria, extending over approximately 15 ha (Malacrino, 2014).

The remains of the villa were already known in the 19th century, but the first systematic excavations began only in 1963, during the construction of the *Cassa del Mezzogiorno* aqueduct, which caused damage

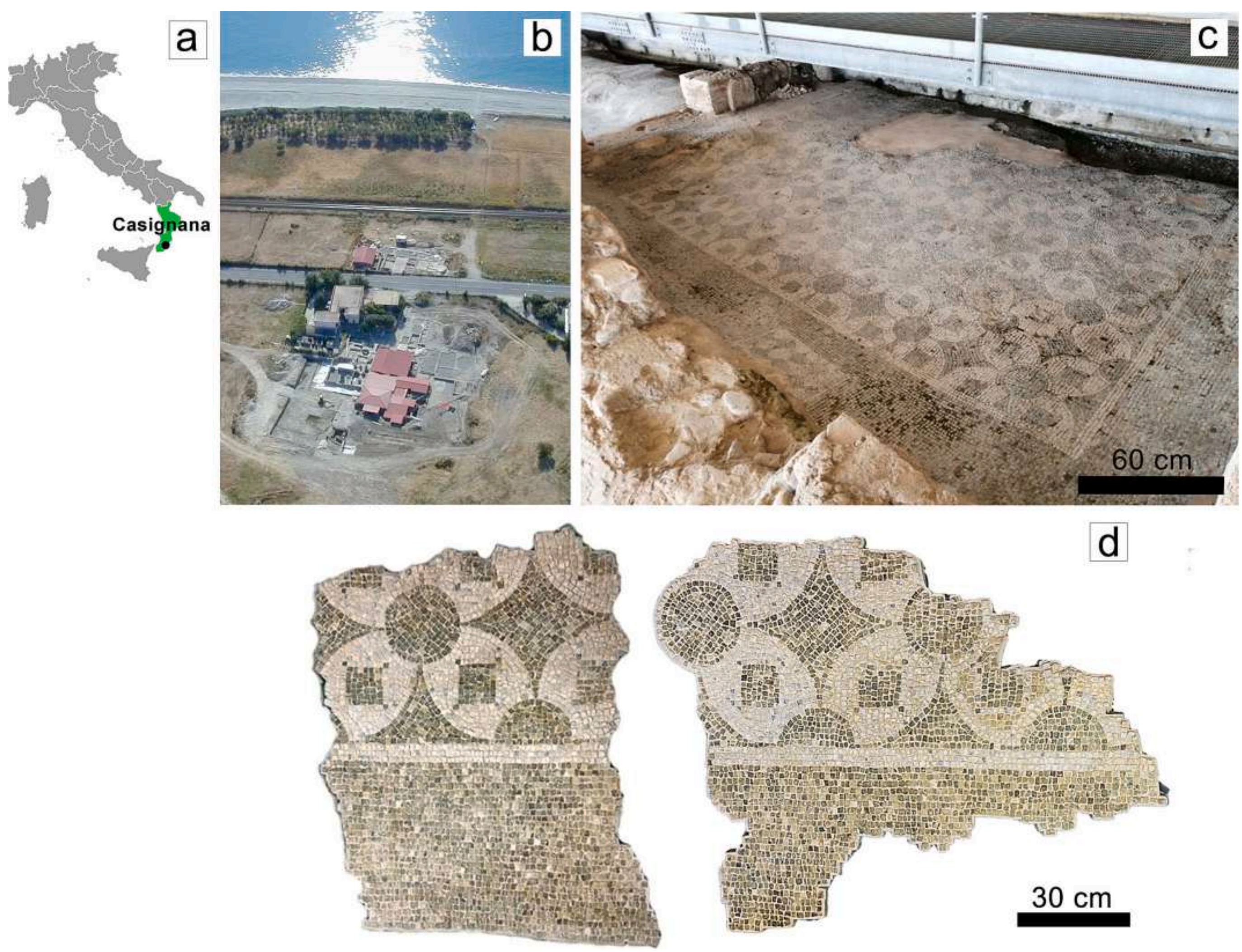

Fig. 1. Images showing: (**a**) the location of Casignana in the Calabria region; (**b**) the view from the aerial view of the archaeological site of Casignana; (**c**) the "*A grandi Fiori*" Mosaic in the residential area of the roman villa; (**d**) the two "*A grandi Fiori*" mosaic fragments detached.

to both the mosaic pavements and the *opus sectile* floors. The northern area of the bath complex was excavated between 1964 and 1966, with further campaigns from 1980 completing its exploration (Sabbione et al., 1997). After limited activity in the 1990s, excavations resumed in 1999, when the Municipality of Casignana acquired the adjacent land, allowing investigations to extend between the SS 106 and the railway and revealing the villa's present configuration.

The roman villa of Casignana is organized around a central courtyard: the baths and service rooms are located to the West and South, the residential area to the East, while the northern part includes structures whose function remains uncertain (Sabbione, 2007). The surrounding area also comprised a monumental fountain and a system of cisterns.

The earliest phase of the villa probably dates back to the 1st century CE but its peak in architectural and decorative development is placed between the 3rd and 4th centuries CE. The villa was abandoned in the 1st half of the 5th century, although the area continued to be frequented until the 7th century (Grillo, 2014).

Renowned for the richness of its decorative program, the villa preserves the largest collection of mosaic floors so far documented in Calabria, with more than 25 rooms decorated with geometric and figural motifs dating back to the 3rd and 4th centuries CE. Although many questions regarding the organization of mosaic craftsmanship in antiquity remain unresolved – such as whether entire pavements were executed by a single workshop or, more plausibly, by multiple mosaicists active on site at different times – what is evident at Casignana is the use of decorative motifs and patterns that circulated among craftsmen and were subsequently adapted to produce personalized variations. The remarkable concentration of high-quality mosaics within a single building constitutes compelling evidence that, in the Late Imperial period, a sophisticated and affluent elite resided in Locri area (Bruni, 2009).

Notable examples include the mosaics of the bath complex depicting sea nymphs riding sea monsters, the geometric compositions in the *caldarium* of the western baths and figurative mosaics in service areas illustrating the triumph of Dionysus (Sabbione et al., 1997). The complexity of both geometric and figural schemes, together with the skilled use of *tesserae* of diverse colours, reflects the high technical expertise of the mosaicists in fulfilling the refined commissions of the *dominus*.

The present investigation focuses on the "*A Grandi Fiori*" mosaic, situated within the residential quarter of the villa, in "Room N" of the residential area of the villa (Fig. 1c). This mosaic floor, datable to the first half of the 3rd century CE, is composed of green and white *tesserae* arranged to form floral motifs with four petals encircling a central green sphere. Each petal contains a small vertically oriented green square, while the juxtaposition of adjacent flowers creates concave green squares at their intersections. The entire composition is enclosed within a frame of green *tesserae* (Bruni, 2009).

The mosaic was discovered in 1999 during excavation campaigns that brought to light six small rooms of the residential area, some of which, including "Room N", had been damaged by the construction of the modern SS106 road (Sabbione, 2007). In the 1960s, following the construction of both the aqueduct and the SS106, portions of the "*A Grandi Fiori*" mosaic were detached and removed from their original contest and stored in the municipal depots of Casignana (Fig. 1d).

3. Sampling and analytical methods

A recent conservation intervention, carried out between 2020 and 2021, allowed the recovery and consolidation of two severely degraded portions of the mosaic "*A Grandi Fiori*". The primary objectives were to secure the fragments, provide a new structural support, and promote their valorisation and public accessibility. In parallel with the conservation work, a diagnostic campaign was carried out. In such contest, *tesserae* samples were systematically collected to enable a comprehensive characterization of the constituent materials and to undertake detailed provenance investigations.

Following a detailed examination of the mosaic surface, a sampling strategy was applied. *Tesserae* that appeared detached, and in some cases did not correspond to existing lacunae within the mosaic, were selected for analysis. Sampling was preceded by macroscopic observation and lithological assessment, which suggested the possible presence of marble and limestone lithotypes, respectively, in the white and green *tesserae*.

Following these lines, twenty-nine samples (five green limestone and twenty-four white marble *tesserae*) representing the primary lithologies were selected for characterization analysis. A comprehensive list and description of the samples is provided in Table 1. At the same time, provenance studies were carried out on the white marble *tesserae*. A multi-analytical approach combining techniques from geoscience, chemistry, and physics was applied to accurately determine the marble provenance, as a single method is insufficient to unequivocally identify the most likely source.

Each *tessera*, having an approximate dimension of 1.5 cm x 1.5 cm, was initially cleaned with pure water and subsequently brushed to remove superficial soil deposits.

When possible, a part of each *tessera* (both white and green) was powdered and analysed by means of X-Ray Diffraction (XRD) while the remaining portion was prepared to obtain the thin sections for Polarized Optical Microscopy (POM) observation and Scanning Electron Microscopy equipped with an Energy Dispersive Spectrometer (SEM-EDS) analyses. In addition, the determination of the stable ^{13}C and ^{18}O isotope composition by Mass Spectroscopy (MS) was conducted on the powdered white marble samples.

POM investigation was carried out on thin sections using a Zeiss AxioLab microscope equipped with a digital camera. The aim was to define the petrographic and mineralogical features of the green and white *tesserae*.

Furthermore, the Maximum Grain Size (MGS) of calcite/dolomite crystals, Boundary Grain Shape (GBS) of carbonate grains and the presence of directional geometric features (anisotropic texture), were considered for the characterization of the white marble *tesserae* (Antonelli and Lazzarini, 2015; Ricca et al., 2015; Capedri and Venturelli, 2004; Gorgoni et al., 2002; Lazzarini et al., 1980). MGS values (mm)

Table 1
Description of the examined mosaic *tesserae* samples and analytical methods.

Sample ID	Colour	Lithotype	Analysis
CM1	Green	Limestone	POM; SEM-EDS
CM2	Green	Limestone	POM; SEM-EDS
CM3a	Green	Limestone	POM; SEM-EDS
CM3b	Green	Limestone	POM; SEM-EDS
CM4	Green	Limestone	POM; XRD
CM5	White/greyish	Marble	POM, XRD, MS, SEM-EDS
CM6	White/greyish	Marble	POM; SEM-EDS
CM7	White/greyish	Marble	POM, XRD, MS, SEM-EDS
CM8	Snow-white	Marble	POM, XRD, MS, SEM-EDS
CM9	White/greyish	Marble	POM, XRD, MS, SEM-EDS
CM10	White	Marble	POM, XRD, MS, SEM-EDS
CM11	White	Marble	POM, XRD, MS, SEM-EDS
CM12	Greyish	Marble	POM, XRD, MS, SEM-EDS
CM13	White/grey, veined	Marble	POM, XRD, MS, SEM-EDS
CM14	White	Marble	POM, XRD, MS, SEM-EDS
CM15	White	Marble	POM, XRD, MS, SEM-EDS
CM16	White	Marble	POM, XRD, MS, SEM-EDS
CM17	Snow-white	Marble	POM, XRD, MS, SEM-EDS
CM18	White/grey, veined	Marble	POM, XRD, MS, SEM-EDS
CM19	White	Marble	POM, XRD, MS, SEM-EDS
CM20	White/grey, veined	Marble	POM, XRD, MS, SEM-EDS
CM21	White	Marble	POM, XRD, MS, SEM-EDS
CM22	White	Marble	POM, XRD, MS, SEM-EDS
CM23	White	Marble	POM, XRD, MS, SEM-EDS
CM24	Greyish	Marble	POM, XRD, MS, SEM-EDS
CM25	White	Marble	POM, XRD, MS, SEM-EDS
CM26	White	Marble	POM, XRD, MS, SEM-EDS
CM27	White/greyish	Marble	POM, XRD, MS, SEM-EDS
CM28	White	Marble	POM, XRD, MS, SEM-EDS

were measured directly on thin-section micrographs. Then, for each sample, the average was calculated from 4 to 5 measurements taken on the largest grains.

The mineralogical composition of the stone *tesserae* was analysed through a PANanalytical X'PERT PRO diffractometer, with the following operating conditions: Cu anode, graphite monochromator, 40 kV and 30 mA, 5-60° scan range, 2° 2θ min–1 scan rate and 2 s time constant for white marble *tesserae* and for selected sample of green stone *tesserae* and white/grey veined marbles.

The measurement of carbon and oxygen stable isotopes ($\delta^{13}C$ and $\delta^{18}O$) was conducted by MS at the mass spectrometry laboratory of the Department of Earth and Marine Sciences of the University of Palermo (Palermo, Italy) on the white marble samples. Analyses were performed using an automated continuous flow carbonate preparation Gas BenchII device and a ThermoElectron Delta Plus XP mass spectrometer. A small amount of powder was heated at 400°C to remove organic components and later subjected to acidification at 50°C. Samples were calibrated to Vienna Pee Belemnite (V-PDB) using an internal standard (Carrara Marble with $\delta^{18}O = -2.43‰$ vs. V-PDB and $\delta^{13}C = 2.43‰$ vs. V-PDB) and NBS19. Standard deviations of oxygen and carbon isotope measures were estimated as 0.08 and 0.1‰ respectively, based on ~ 100 repeated samples. All isotope data were reported in per mil (‰) relative to the V-PDB standard.

Finally, SEM-EDS was performed to investigate the elemental profile and, more in detail, the presence of accessory minerals especially in marble *tesserae*. Indeed, the distribution of accessory phases in white marbles is not always homogeneous, and in some cases the presence of specific minor constituents and their relative abundance can be decisive in discriminating the source quarries (Capedri and Venturelli, 2004; Capedri et al., 2004). The scanning electron microscope was an Ultra-high-resolution SEM (UHR-SEM)—ZEISS Cross-Beam 350 equipment, coupled with the spectrometer EDS-EDAX OCTANE Elite Plus-Silicon drift type. Instrumental conditions set for EDS analyses were HV: 15 keV and probe current: 100 pA.

4. Results and discussion

4.1. Green tesserae

Based on microscopic observation under POM, the green *tesserae* (CM1, CM2, CM3a, CM3b, CM4) are limestones exhibiting isotropic to slightly anisotropic textures (Fig. 2a, b). Allochems, mainly represented by microfossils, constitute approximately 10% of the rock volume, although slight variations in their distribution are observed. Bioclasts are rarely in contact, generally separated by a micritic matrix, and most likely consist of planktonic foraminifera (*Globigerinidae* family) (Fig. 2d) and the calcitic models of radiolarians (Fig. 2c). In all samples, numerous unoriented veins filled with mosaics of coarser calcite crystals are present (Fig. 2b). According to the classifications of Folk (1962) and Dunham (1962), the samples can be described as biomicrite and mudstone, respectively.

XRD investigation revealed a predominantly calcitic composition, with subordinate amounts of quartz and clay minerals (Fig. 3). Moreover, alteration phases attributable to calcium oxalates (whewellite) were identified. These phases are most probably related to the metabolic activity of biodeteriogenic organisms and/or to the transformation of organic compounds used as adhesives for the application of the facing fabric during the detachment of the mosaics (Rampazzi, 2019).

The mineralogical data are corroborated by SEM–EDS analyses (Table 2). Moreover, chemical microanalyses revealed high iron contents and the presence of iron oxides and sulphides, which are most likely responsible for the green coloration of the *tesserae* (Fig. 4a, b). In addition, titanium oxides were identified as secondary mineral phases.

The minero-petrographic features of the green *tesserae* appear comparable to the greenish-greys biomicritic levels of the Variegated Clays Formation, dated to the Cretaceous-Lower Miocene, and widely

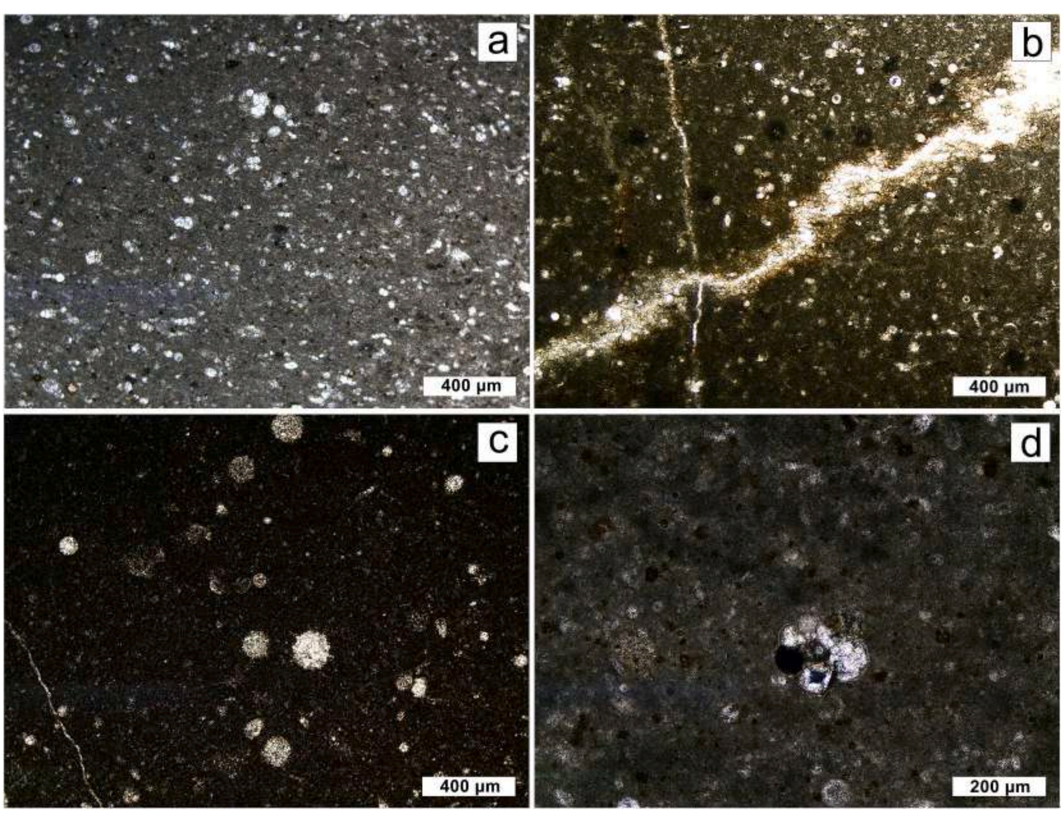

Fig. 2. Representative photomicrographs (crossed-polarised light) of the thin sections obtained from the green limestone samples showing: (**a**) the textural and compositional features of the lithotype (sample CM3a); (**b**) calcite veins (sample CM1); (**c**) radiolarians (sample CM3b); (**d**) planktonic foraminifera (sample CM4).

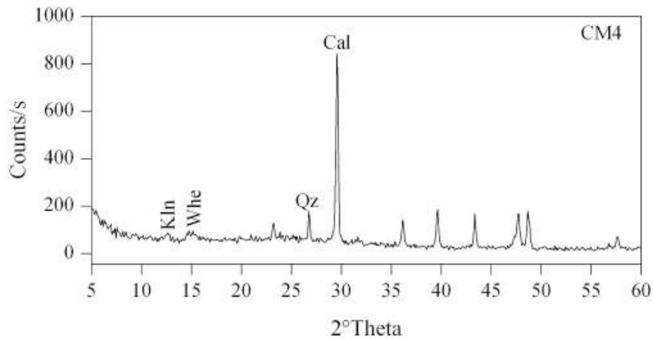

Fig. 3. XRD pattern representative of the green micritic *tesserae* (sample CM4). Legend: Qz = quartz; Cal = calcite; Kln = kaolinite; Whe = whewellite.

outcropping around Casignana (Critelli et al., 2016; Cavazza and Barone, 2010), suggesting a probable local provenance of the materials. However, future more in-depth studies are planned, in order to further investigate this hypothesis, starting with the identification and comparison of the microfossil associations in the *tesserae* samples and in the local rock outcrops.

4.2. *White tesserae*

4.2.1. *Polarising optical microscopy and x-ray diffraction analysis*

The results of the petrographic investigation are summarized in Table 3 and illustrated in Fig. 5a, b, c, d, e, f, g while representative XRD spectra of white/greyish and white marble samples are shown in Fig. 6a, b. Based on thin-section microscopic observation and mineralogical characteristics, the samples can be subdivided into two distinct groups according to their maximum grain size (MGS). The MGS is considered an important diagnostic parameter for a preliminary discrimination of the provenance of white marbles. It is generally related to the metamorphic history that governed marble formation and is commonly proportional to its metamorphic grade (the higher the MGS, the higher the grade, all other conditions being equal) (Antonelli and Lazzarini, 2015; Moens et al., 1988).

A first group, consisting of 15 samples (CM5, CM6, CM7, CM8, CM9, CM10, CM11, CM12, CM14, CM19, CM21, CM22, CM24, CM25, and CM26), is composed of medium-grained marbles with MGS values mostly around 2 mm (ranging between 1.45 mm and 3.25 mm).

The fabric of samples CM5, CM6, CM7, CM8, CM9, CM11, CM14, CM19, CM21, CM22, CM24, CM25, and CM26 is markedly heteroblastic (He), with a characteristic mortar microstructure (Mo), in which larger calcite crystals are surrounded by smaller ones formed through deformation and subsequent recrystallization (Fig. 5a). In some cases, specifically samples CM5, CM14, CM22, and CM26, the microstructure is only weakly mortar-like, locally trending toward a mosaic fabric. The vast majority of carbonate crystals display clear polysynthetic twinning and rhombohedral cleavage. Evidence of strain is also expressed through numerous distortions of the twin lamellae. The grain boundary shape (GBS) of the carbonate crystals ranges from curved and embayed to sutured (Cu/Emb; Su), while 120° triple junctions are only rarely observed. No preferred orientation is detected, and the overall texture may therefore be defined as isotropic (I). Furthermore, sample CM9 contains a vein characterized by very fine-grained, equidimensional calcite and dolomite crystals so tightly intergrown that the GBS is locally indistinguishable.

Among the accessory minerals observed petrographically, opaques occur sporadically. From a mineralogical perspective, all samples are purely calcitic except samples CM9, in which calcite is subordinate to

Table 2
Values of the main oxides (wt.%) determined through SEM-EDS analysis on the matrix and crystals within the green micritic samples.

Sample ID	Analysis type	Area	Na_2O	MgO	Al_2O_3	SiO_2	SO_3	K_2O	CaO	MnO	FeO	TiO_2	Tot
CM1	Area	Matrix	0.5	3.6	7.6	22.3	–	0.7	55.3	–	10.0	–	100
	Area	Fe-ox/sulph crystal	3.0	1.5	1.6	8.8	13.1	–	15.0	–	57.0	–	100
	Spot	Ti-ox crystal	–	–	2.7	7.1	–	–	3.4	–	–	86.8	100
CM2	Area	Matrix	–	3.2	5.5	24.9	–	0.5	58.8	–	7.2	–	100.1
CM3b	Area	Matrix	0.3	1.8	3.4	15.6	–	0.6	71.7	0.6	6.1	–	100.1
CM3a	Area	Matrix	0.8	3.4	7.3	27.1	–	0.8	53.6	–	6.9	–	99.9

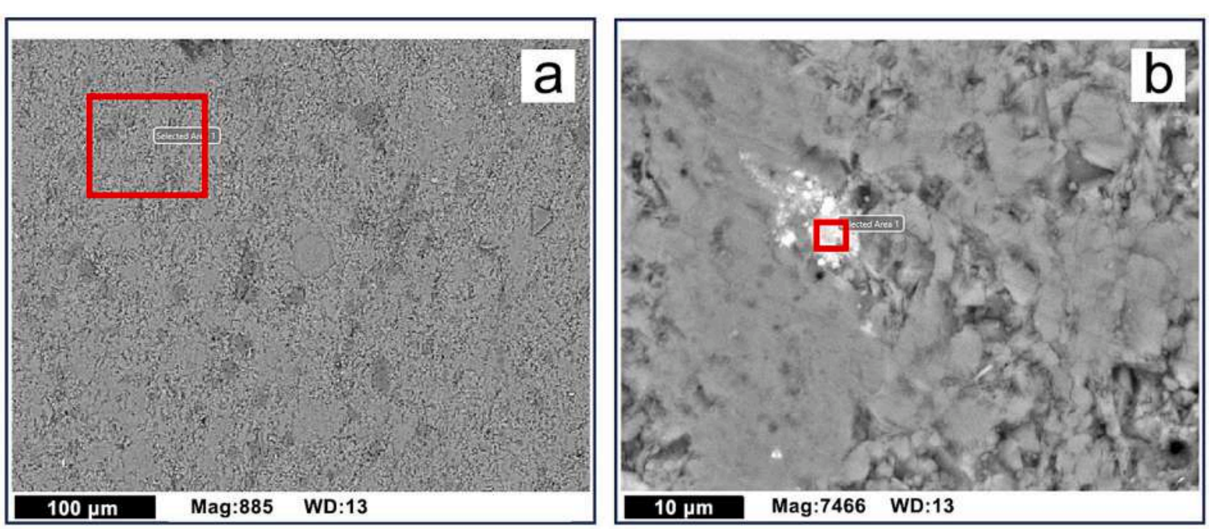

Fig. 4. SEM-BSE images showing the analysis areas (red squares) performed on (**a**) the matrix and on the (**b**) Fe-oxides/sulphides crystals of the green limestone sample CM1.

Table 3
List of the minero-petrographic features of the white marble *tesserae* under analysis. Legend: He = heteroblastic; Ho = homeoblastic; Mo = mortar; W-Mo = weakly mortar; G = granoblastic; P = polygonal; St = straight; Cu = curved; Emb = embayed; Su = sutured; W-An = weakly anisotropic; I = isotropic; Cal = calcite; Dol = dolomite; +++ = prevalent; ++ = abundant; tr = traces.

Sample ID	Fabric type	Microstructure	MGS (mm)	GBS	Anisotropic/isotropic texture	Mineralogical composition
CM5	He	W-Mo	3.25	St, Cu	I	Cal (+++)
CM6	He	Mo	2.15	Cu/Emb, Su	I	–
CM7	He	Mo	2.59	Su, Emb	I	Cal (+++)
CM8	He	Mo	2.57	Cu/Emb, Su	I	Cal (+++)
CM9	He	Mo	2.27	Cu/Emb, Su	I	Dol (+++) Cal (++)
CM10	Ho	G	2.16	St, Cu/Su	W-An	Cal (+++) Dol (++)
CM11	He	Mo	1.80	Cu/Emb, Su	I	Cal (+++)
CM12	Ho	G	2.08	Cu/Emb, Su	I	Cal (+++) Dol (++)
CM13	He	G	1.37	Emb, Cu	W-An	Cal (+++)
CM14	He	W-Mo	2.01	Cu/Emb, Su	I	Cal (+++)
CM15	He	G, strained	1.32	Emb	W-An	Cal (+++)
CM16	W-He	G, strained	0.84	Emb	W-An	Cal (+++)
CM17	Ho	G	1.36	Cu/Su	W-An	Cal (+++)
CM18	Ho/He	G, strained	1.15	Emb	I	Cal (+++)
CM19	He	Mo	2.39	Cu/Emb, Su	I	Cal (+++)
CM20	Ho	G	1.27	Emb, Cu	W-An	Cal (+++)
CM21	He	Mo	2.52	Cu/Emb, Su	I	Cal (+++)
CM22	He	W-Mo	1.95	Cu/Emb, Su	I	Cal (+++)
CM23	Ho	P	0.88	St, Cu	I	Cal (+++)
CM24	He	Mo	1.45	Su	I	Cal (+++) Dol (tr)
CM25	He	Mo	2.58	Cu/Emb, Su	I	Cal (+++) Dol (tr)
CM26	He/Ho	W-Mo	2.33	Cu/Emb, Su	I	Cal (+++)
CM27	He	G	1.27	Emb	W-An	Cal (+++) Dol (tr)
CM28	He	G	6.90	Emb, Su	I	Cal (+++)

dolomite, and sample CM25 and CM24, in which dolomite occurs only in trace amounts.

Within the medium-grained marbles, two samples exhibit textural characteristics distinctly different from those described above.

Sample CM10 (MGS = 2.16 mm) is a medium-grained marble characterized by a mosaic microstructure (G), with equidimensional carbonate crystals (Ho) and a slight preferred orientation (W-An) (Fig. 5b). Post-crystalline deformation features are virtually absent. Polysynthetic twinning and rhombohedral cleavage are clearly visible in the carbonate grains. Elongated clusters of small carbonate crystals occur sporadically. Grain boundaries vary from straight to curved to sutured (St; Cu/Su). Frequent euhedral opaques were identified as accessory phases and mineralogical analyses revealed the presence of both calcite and dolomite.

Sample CM12 (MGS = 2.08 mm), by contrast, is a granoblastic marble (G) with a predominantly homeoblastic fabric (Ho) and fine-grained texture (0.1–0.2 mm) (Fig. 5c). However, sporadic calcite porphyroblasts of markedly larger size (ca. 2 mm) are present. The GBS is typically curved and embayed, with the larger grains sometimes showing sutured boundaries (Cu/Emb, Su). Occasional polysynthetic twinning and rhombohedral cleavage are present, and no preferred orientation is observed (I). Opaques occur infrequently and the mineralogical composition consists of calcite with subordinate dolomite.

The second group consists of eight samples (CM13, CM15, CM16, CM17, CM18, CM20, CM23, and CM27) characterized by a fine grain size (MGS between 0.84 and 1.36 mm).

Samples CM13, CM15, CM16, CM17, CM18, and CM27 exhibit a fabric ranging from heteroblastic (He) to homeoblastic (Ho), often characterized by a slight foliation of the carbonate crystals (W-An) (Fig. 5d). The microstructure is distinctly mosaic (G) and displays significant intracrystalline deformation, reflected by the distorted polysynthetic twin lamellae and the characteristic undulous extinction of calcite crystals. Carbonate grain boundaries are predominantly embayed (Emb), although curved to sutured GBS (Cu/Su) were occasionally observed. The samples are purely calcitic, with traces of dolomite detected only in sample CM27. Apart from carbonate grains, opaques are extremely rare in thin sections.

Sample CM23, in contrast, is a marble (MGS = 0.88 mm) with a homeoblastic fabric (Ho) and a distinctly polygonal microstructure (P), characterized by triple junctions between carbonate crystals meeting at 120° (Fig. 5e). The GBS ranges from straight to curved (St, Cu), and no preferred orientation is observed. No accessory minerals are visible and the composition is purely calcitic.

Sample CM20 exhibits minero-petrographic features that differ from the other samples in its group. It displays a texture characterized by equidimensional calcite crystals (Ho) and a mosaic microstructure (G), locally with slight foliation (W-An) (Fig. 5f). In some areas, clusters of very fine-grained, highly intergrown carbonate crystals are observed, often associated with abundant quartz, opaques and micas displaying a marked *iso*-orientation. Carbonate grain boundaries vary from curved to embayed (Cu, Emb).

Among all samples examined, only one coarse-grained marble was identified: sample CM28 (MGS = 6.90 mm). This sample, which therefore does not fall into either of the two groups described above, exhibits a heteroblastic fabric (He) with a mosaic microstructure (G) and GBS ranging from embayed to sutured (Emb, Su) (Fig. 5g). Polysynthetic twinning in calcite crystals is frequent and often distorted, while the crystals themselves exhibit clear undulous extinction. No preferred crystal orientation is observed (I), and no accessory minerals are present.

The MGS values of the carbonate grains measured in all analysed samples were compared with literature data relating to the MGS of the white marbles most widely employed in the Mediterranean area during the Roman period (Fig. 7). Only sample CM28 shows an MGS value that falls exclusively within the internal box bar of the Naxos quarry, although compatibility with the Thasos-2 district cannot be entirely excluded, considering the high MGS values occasionally observed in quarry samples from the Phanari district (Attanasio et al., 2006).

For the remaining samples, due to the extensive overlap of the box bars, it is not possible to determine provenance with certainty. Indeed, marble samples with MGS between 0.84 and 1.36 mm (CM13, CM15, CM16, CM17, CM18, CM20, CM23, and CM27) fall generally within the field of fine-grained marbles (Carrara, Göktepe, Docimium, Pentelicon, Hymettos, and Paros Marathi), whereas samples with MGS between 1.45 and 3.25 mm (CM5, CM6, CM7, CM8, CM9, CM10, CM11, CM12, CM14, CM19, CM21, CM22, CM24, CM25, and CM26) are consistent with marbles typically classified as medium-grained (Aphrodisian, Proconnesian, Parian Chorodaki and Thasian Vathy-Saliara). Although

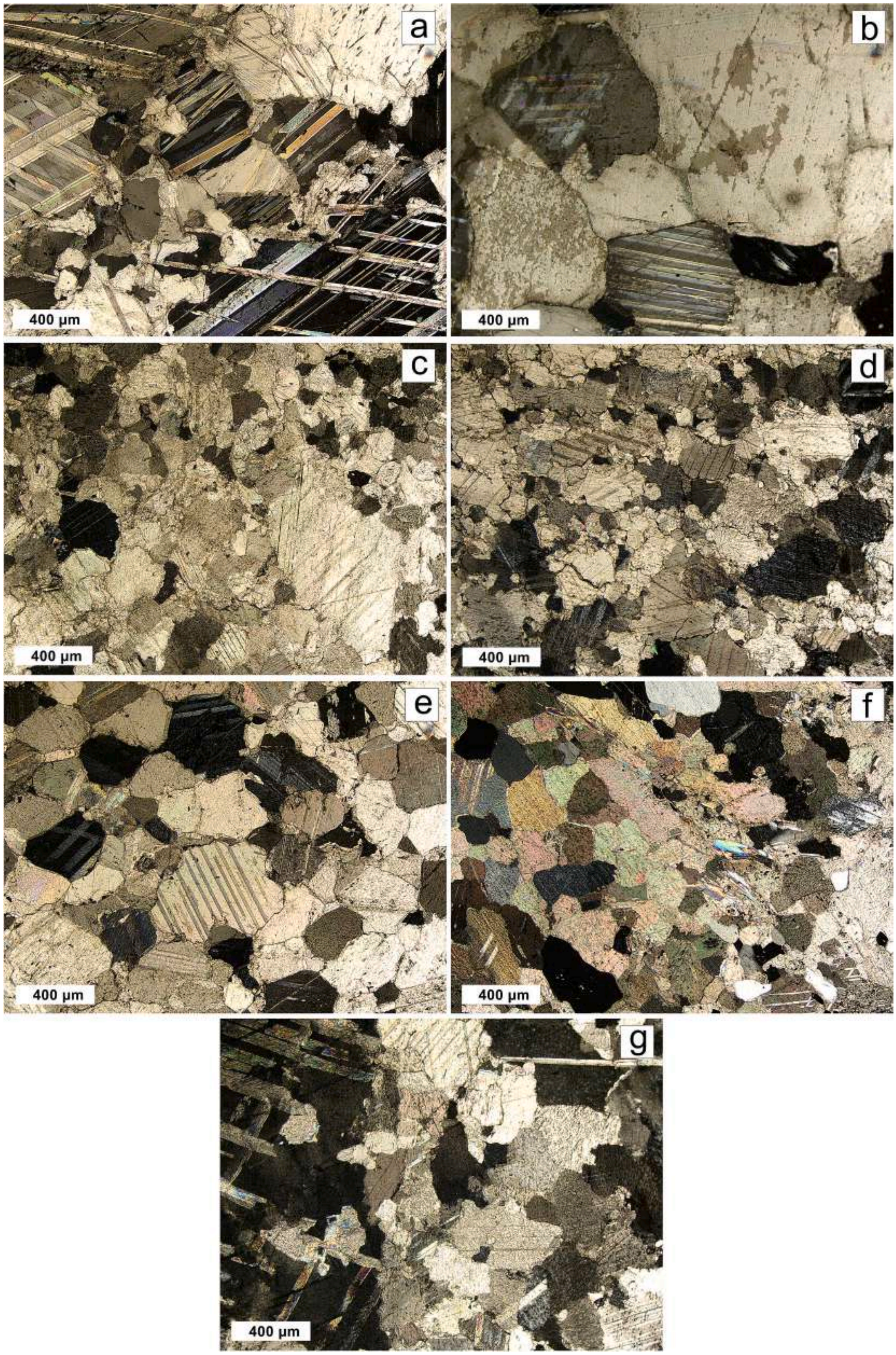

Fig. 5. Representative photomicrographs showing textural features of some marble samples (cross-polarized light): (**a**) average-grained heteroblastic marble with typical mortar microstructure of sample CM7; (**b**) homeoblastic marble (sample CM10) with a mosaic microstructure with straight to curved to sutured GBS; (**c**) granoblastic marble with a predominantly homeoblastic fabric and fine-grained texture (sample CM12); (**d**) fine-grained marble with heteroblastic to homeoblastic fabric and embayed GBS, characterized by a slight foliation of the carbonate crystals (sample CM16); (**e**) fine-grained homeoblastic marble and polygonal microstructure, with triple junctions between carbonate crystals (sample CM23); (**f**) mosaic microstructure of fine-grained marble CM20, locally with slight foliation showing quartz, opaques and oriented micas; (**g**) strongly heteroblastic coarse-grained marble with a mosaic microstructure and embayed to sutured GBS of sample CM28.

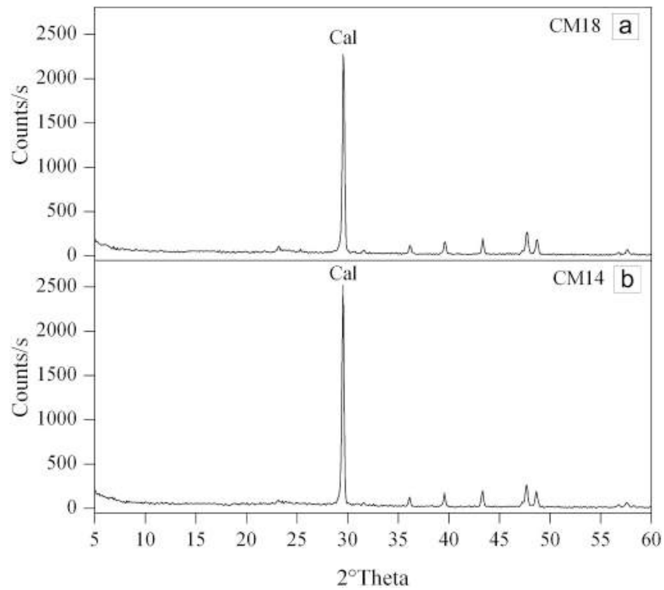

Fig. 6. Representative XRD spectra of both (**a**) white/greyish (CM18 sample) and (**b**) white (CM14 sample) marble *tesserae*. Legend: Cal: calcite.

petrographic thin-section analysis alone provides only preliminary information, these data become diagnostically fundamental when combined with stable C and O isotope ratio analysis.

4.2.2. Isotopic measurements

The isotopic measurements of $\delta^{13}C$ and $\delta^{18}O$ obtained from the white marble samples are reported in Table 4 and plotted within the two most updated isotopic reference diagrams for fine-grained marbles and for medium- to coarse-grained marbles (Fig. 8a,b) (Maniatis et al., 2024; Prochaska, 2023; Prochaska and Attanasio, 2022; Prochaska and Attanasio, 2021; Musso et al., 2018; Attanasio et al., 2008; Attanasio et al., 2006).

The medium- and coarse-grained samples (CM5, CM7, CM8, CM9, CM10, CM11, CM12, CM14, CM19, CM21, CM22, CM24, CM25, CM26, CM28) display rather homogeneous isotopic values, falling within a range of − 0.57 to − 2.74‰ for $\delta^{18}O$ and 3.75 to 2.39‰ for $\delta^{13}C$. Only samples CM19 and CM28 exhibit more negative $\delta^{18}O$ values (Fig. 8a).

Specifically, sample CM7 falls exclusively within the Proconnesos-1 field (Saraylar district), in an area very close to the Thasos Aliki domain; samples CM5, CM11, CM14, CM22, and CM25 are included within both the Proconnesos-1 and Thasos Aliki fields; sample CM8 plots in the Thasos Aliki domain, at the boundary with Proconnesos-1; sample CM19 is compatible with the Proconnesos-2 (Camlik quarry district) and Thasos Vathy-Saliara fields; isotopic signature of sample CM21 is consistent with the Proconnesos-1, Paros Marathi *non-lychnites*, and Thasos Aliki domains, while sample CM9, in addition to these, shows affinity with the Thasos Acropolis/Phanari quarry and sample CM26 also fits into the Paros Chorodaki and Thasos Acropolis/Phanari fields too; samples CM12 and CM24 fall within an area where the Proconnesos-1, Paros Marathi *non-lychnites*, and Aphrodisias-1 (City Quarries) domains overlap; sample CM28 lies within the Naxos, Aphrodisias-1 and Thasos Acropolis/Phanari quarries.

Although sample CM10 exhibits an MGS > 2 mm, it shows a $\delta^{13}C$ value higher than 4‰, placing it outside the isotopic fields defined by the reference diagrams for medium to coarse-grained marbles. Therefore, it may correspond to an atypical variety of fine-grained marble characterized by an unusually large MGS, considering that its MGS is only slightly above 2 mm (MGS = 2.16 mm). When plotted in the diagram for fine-grained marbles, its isotopic values fall within a region compatible with Paros Marathi *lychnites*.

The fine-grained samples (CM13, CM15, CM16, CM17, CM18, CM20, CM23, and CM27) instead display a rather broad distribution of $\delta^{13}C$ and $\delta^{18}O$ values (Fig. 8b). In particular, sample CM27 exclusively lies within the Docimium domain; samples CM15, CM16 and CM18 are consistent with the Docimium and Göktepe fields, while sample CM13, in addition to these, also matches the Paros Marathi *lychnites* domain; sample CM17 fits within the Penteli and Docimium districts; sample CM23 plots in a region where the Carrara, Hymettos, and Docimium domains intersect.

Regarding sample CM20, an affinity with the Penteli district cannot be excluded. A recent study of $\delta^{13}C$ and $\delta^{18}O$ stable isotopes conducted on Pentelic quarry samples expanded the 90% probability ellipsoid defined in previous studies, extending the distribution of isotopic values towards higher $\delta^{13}C$ values (Pike, 2025). When the isotopic values of sample CM20 are re-plotted in these updated diagrams, it becomes

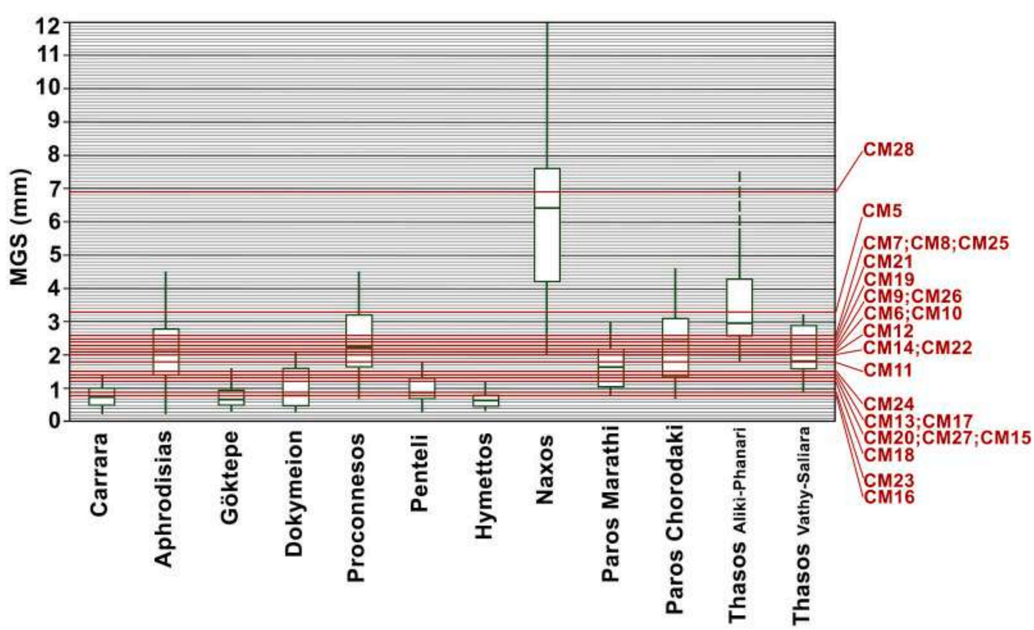

Fig. 7. Diagram of the maximum grain size (MGS) values measured in the analysed marbles compared with those of the most used Mediterranean white marbles used in antiquity. Modified from Antonelli and Lazzarini (2015).

Table 4
Isotopic data of the investigated white marble samples and probable provenance according to the isotopic signature.

Sample ID	$\delta^{13}C$	$\delta^{18}O$	Probable provenance
CM5	3.57	−0.99	Proconnesos-1, Thasos Aliki
CM7	3.75	−1.39	Proconnesos-1
CM8	3.65	−0.57	Thasos Aliki, Proconnesos-1
CM9	2.61	−1.42	Proconnesos-1, Paros Marathi *non-lychnites*, Thasos Aliki, Thasos Acropolis/Phanari
CM10	4.71	−2.81	Paros Marathi *lychnites*
CM11	2.97	−0.65	Proconnesos-1, Thasos Aliki
CM12	2.99	−2.74	Proconnesos-1, Paros Marathi *non-lychnites*, Aphrodisias-1
CM13	3.34	−2.81	Docimium, Göktepe, Paros Marathi *lychnites*
CM14	3.49	−1.32	Proconnesos-1, Thasos Aliki
CM15	0.48	−3.28	Docimium, Göktepe
CM16	2.61	−3.98	Docimium, Göktepe
CM17	2.74	−6.00	Penteli, Docimium
CM18	3.54	−2.55	Docimium, Göktepe
CM19	3.15	−6.89	Proconnesos-2, Thasos Vathy/Saliara
CM20	4.38	−6.20	Penteli
CM21	3.16	−1.72	Proconnesos-1, Paros Marathi *non-lychnites*, Thasos Aliki
CM22	3.26	−1.13	Proconnesos-1, Thasos Aliki
CM23	2.46	−1.60	Carrara, Hymettos, Docimium
CM24	2.86	−2.22	Proconnesos-1, Paros Marathi *non-lychnites*, Aphrodisias-1
CM25	3.46	−1.21	Proconnesos-1, Thasos Aliki
CM26	2.39	−1.28	Proconnesos-1, Paros Marathi *non-lychnites*, Thasos Aliki, Paros Chorodaki, Thasos Acropolis/Phanari
CM27	2.65	−4.28	Docimium
CM28	1.84	−4.44	Naxos, Aphrodisias-1, Thasos Acropolis/Phanari

evident that the sample is also compatible with the Pentelic archaeological quarries located on the lower slope of Marble Unit 3 (Fig. 9).

4.2.2.1. SEM-EDS investigation. SEM-EDS analyses were carried out to identify and characterize accessory minerals present in the nine microfragments investigated. Although many of them are relatively common across the examined varieties, the identification of specific mineralogical phases, when integrated with isotopic analyses and petrographic observations, have proved to be crucial for determining the provenance of the archaeological marbles.

The accessory phases observed in this study, together with their distribution, are listed in Table 5. The identified accessory minerals were compared with those reported in the literature for the main Mediterranean quarrying districts exploited in antiquity and accordingly, the most probable provenance has been proposed (Capedri et al., 2004; Capedri and Venturelli, 2004).

The majority of the samples contains dolomite, either in trace amounts or as a subordinate phase to calcite, with the exception of samples CM5, CM13, CM14, CM15, CM18, CM22, CM23, CM27 and CM28. Its occurrence is often ubiquitous in white marbles, with the notable exception of the Naxos and Paros quarries, where it is absent.

The predominant non-carbonate accessory phase in almost all analysed samples is fluorapatite. The crystals are typically rounded and very small, ranging from 10 to 40 μm. Such features are generally observed in Carrara, Penteli, Paros, Proconnesos, and Aphrodisias marbles. Conversely, larger fluorapatite grains (50–100 μm) were detected in samples CM5, CM7, CM9, CM13, CM14, CM19, CM25 and CM26, which is indicative of Naxos and Thasos areas.

Quartz was identified as a few small grains (20–30 μm) in samples CM13 and CM18. Only sample CM20 contains numerous detrital quartz crystals reaching 200 μm. This phase is observed in the Docimium and Aphrodisias districts, although it becomes abundant in marbles from Carrara and Pentelicon.

Samples CM6, CM11, CM13, CM18, CM21, and CM26 also exhibit albitic plagioclase crystals. In samples CM13, CM18, and CM26, these crystals are relatively frequent and of moderate size (generally up to 50 μm), although larger individuals (100–300 μm) are also present. In samples CM6, CM11, and CM21 they occur sporadically and are generally around 100 μm in size. According to the literature, plagioclase crystals have been reported in the Aphrodisias and Carrara quarrying areas.

Sulfides are very common in all analysed samples except for samples CM5, CM8, CM25, and CM28. Most are fine-grained Fe-sulphides (< 20 μm), although in some samples (CM10, CM18, CM19, and CM20) grains reach significant sizes of approximately 100 μm, a feature associated with Carrara, Naxos, Pentelicon, Proconnesos, and Thasos marbles. Zn-sulphide crystals were also occasionally detected in samples CM9, CM11, and CM26, measuring between 5 and 20 μm, compatible with marbles from Thasos.

The oxides observed in the samples consist of iron and titanium oxides. Samples CM11, CM15, CM19, CM21, CM22, CM26, and CM27 exhibit hematite crystals generally < 20 μm, whereas in samples CM16, CM18, and CM20 the grains reach considerable sizes (40–100 μm). Their presence has been reported in Carrara, Penteli, Naxos, Docimium, and Aphrodisias marbles. Titanium oxides, although less frequent, were identified in samples CM9, CM13, CM14, CM16, CM18, CM20, and CM27 as grains < 20 μm, compatible with the Paros, Naxos, Thasos, Proconnesos, and Aphrodisias districts.

Small titanite grains (ca. 30 μm) occur more rarely and were found in samples CM10, CM19, and CM22, whereas fluorite (< 20 μm) was detected in samples CM12, CM16, and CM27. The presence of the latter phase is strongly indicative of Anatolian marbles.

Micas are frequently present in the samples, with crystal sizes ranging from small flakes to, in some cases, 500 μm. Muscovite is the most abundant mica, occurring in samples CM6, CM13, CM16, CM17, CM18, CM19, CM20, CM21, CM24, CM25, and CM27. Phlogopite crystals are also relatively common and were identified in samples CM5, CM6, CM9, CM11, CM19, CM20, CM21, CM22, CM24, CM25, and CM26, a mineral phase often found in Proconnesos, Naxos, Paros, and Thasos marbles. Margarite is less frequently observed (samples CM7, CM22, and CM24), while paragonite occurs in samples CM17, CM21, and CM26. Whereas margarite is characteristic of the Proconnesos district, the presence of paragonite appears consistent with marbles from Paros, Naxos, Thasos, Proconnesos, and Aphrodisias.

Low-temperature phyllosilicates such as chlorite were found exclusively in sample CM17, suggesting Docimium, Carrara, Naxos, Thasos, or Penteli as possible provenance sources for this sample.

4.2.2.2. Final remarks on the marbles' provenance and archaeological considerations. Based on the mineralogical and petrographic features, the isotopic signatures of all samples, and the accessory phases identified by SEM–EDS, integrated with literature datasets on the most commonly used white marbles of the ancient Mediterranean, it was possible to determine the provenance of the marble *tesserae* employed in the "*A Grandi Fiori*" mosaic of the Roman Villa of Casignana (RC, Italy) (Table 6).

- The *tesserae* samples CM5, CM6, CM7, CM8, CM9, CM11, CM12, CM14, CM19, CM21, CM22, CM24, CM25 and CM26 are medium-grained marbles with MGS values consistent with several Mediterranean sources, including Aphrodisias, Proconnesos, Paros Marathi (both *lychnites* and *non-lychnites*), Paros Chorodaki, and Thasos (Phanari, Aliki and Vathy–Saliara), according to the diagram proposed by Antonelli and Lazzarini (Antonelli and Lazzarini, 2015). However, geochemical investigations were essential in excluding several quarrying districts that did not show isotopic affinity. In particular, sample CM7 falls exclusively within the Proconnesos-1 domain (Saraylar district). The textural and mineralogical characteristics, together with the presence of margarite observed under SEM–EDS, corroborate this attribution. Regarding samples CM5, CM8, CM11, CM14, CM22 and CM25, these lie within both the

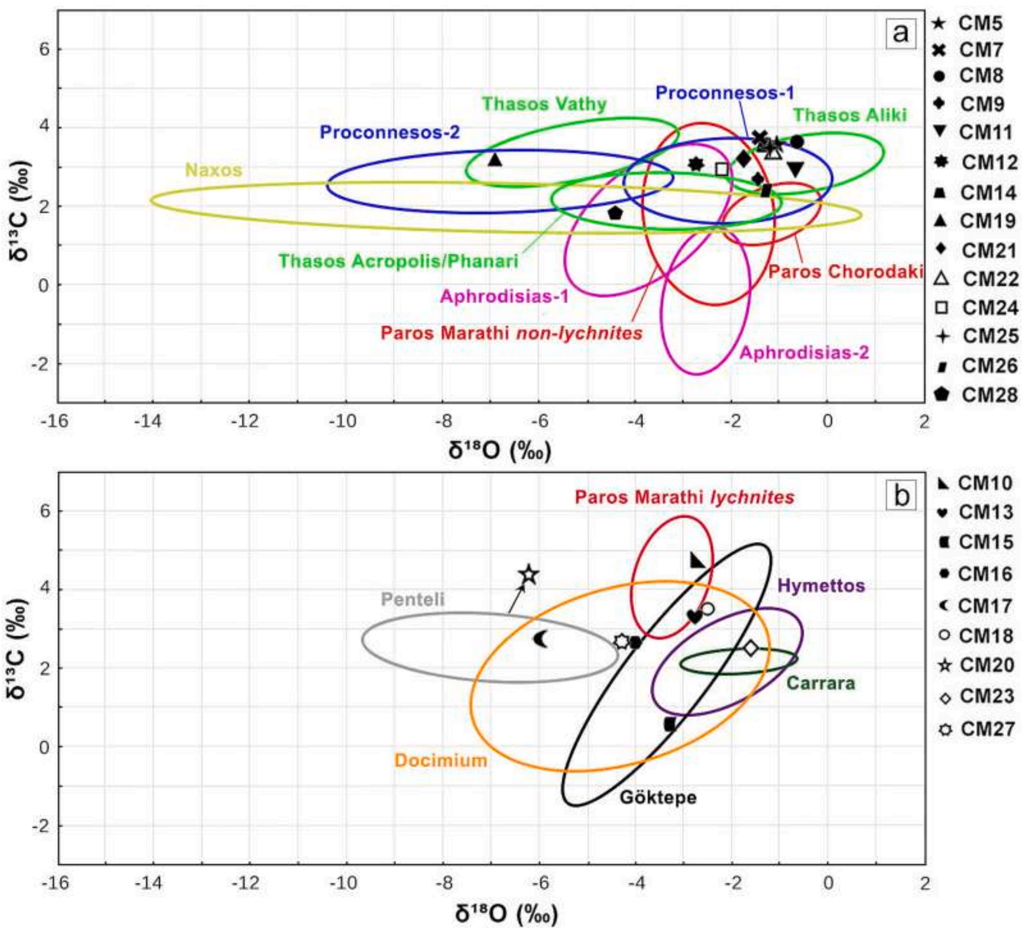

Fig. 8. Isotopic signatures of the white marble samples, plotted against ancient (a) average- to coarse-grained marbles and (b) fine-grained marbles fields. Modified from Maniatis et al. (2024), Prochaska (2023), Prochaska and Attanasio (2022), Prochaska and Attanasio (2021), Musso et al. (2018), Attanasio et al. (2008), Attanasio et al. (2006).

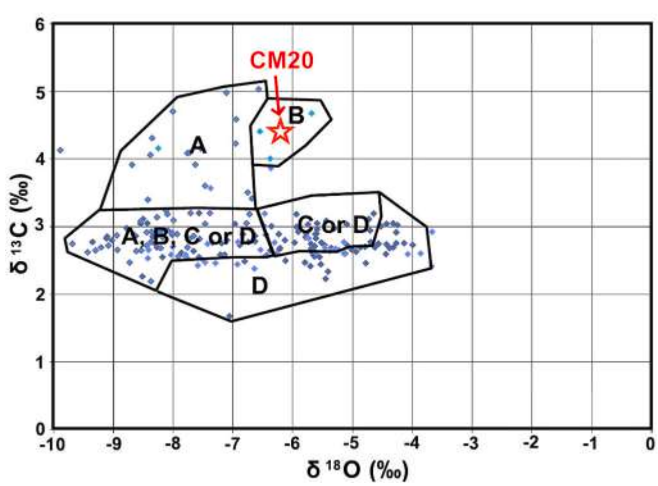

Fig. 9. Isotopic composition of sample CM20 plotted on the isotope diagram of Pentelic marble, with the isotopically defined sub-regions of the marble units outlined: A, Marble Unit 2; B, lower section of Marble Unit 3; C, middle slope of Marble Unit 3; D, upper slope of Marble Unit 3. Modified from Pike (2025).

Proconnesos-1 and Thasos Aliki isotopic fields. The presence of Ti-oxides and Fe-oxides in CM14 and, again, margarite in CM22, both absent in marbles originating from Thasos, allowed the exclusion of the Thasian quarries for these samples, pointing instead to Proconnesos-1 as the most probable source. Samples CM5, CM8, CM11 and CM25 show accessory minerals that are either non-diagnostic or appear common to both quarrying districts. In these cases, a Thasian origin can nonetheless be rejected on the petrographic basis. Although the holotypic Thasos Aliki variety generally exhibits a heteroblastic fabric, the microstructure of these samples is of the “mortar-like” type rather than “mosaic” and lacks accessory phases such as serpentinite, epidote and titanite, typically associated with the Thasos district. For these reasons, CM5, CM8, CM11 and CM25 are also most likely assignable to the Proconnesos-1 quarry. Sample CM19 shows an isotopic signature compatible with the Proconnesos-2 area (Camlik quarry district) as well as Thasos Vathy–Saliara. The latter may be excluded, however, considering the predominantly dolomitic composition of the Vathy–Saliara variety, whereas in the investigated sample dolomite occurs only as an accessory phase. Sample CM21 is isotopically consistent with the domains of Proconnesos-1, Paros Marathi *non-lychnites* and Thasos Aliki, while sample CM26 is also compatible with Paros Chorodaki and Thasos Acropolis/Phanari and CM9 with Thasos Acropolis/Phanari domain too. In these cases, Proconnesos-1 appears again to be the most likely provenance, given the presence of phlogopite and Ti-oxides in CM9, paragonite, phlogopite and dolomite in CM21, and phlogopite and paragonite in CM26. For sample CM24, the presence of margarite allowed exclusion of Paros Marathi *non-lychnites* and Aphrodisias-1, most likely pointing toward a Proconnesian origin. For sample CM6, the small size of the *tessera* did not allow the preparation of sufficient powder for isotopic and mineralogical analysis. From the combination of MGS values, petrographic

Table 5
Accessory minerals occurring in the analysed marble samples observed under SEM-EDS. The plus sign indicates their relative abundance. Legend: Ab = albite; Qz = quartz; F-Ap = fluorapatite; Fe-su = Fe-sulphide; Zn-su = Zn-sulphide; Ti = titanite; F = fluorite; Fe-ox = Fe-oxide; Ti-ox = titanium oxide; Ch = chlorite; Mu = muscovite; Ph = phlogopite; Pa = paragonite; Ma = margarite, Dol = dolomite; +++ very abundant; ++ abundant; + present.

Sample ID	Ab	Qz	F-Ap	Fe-su	Zn-su	Ti	F	Fe-ox	Ti-ox	Ch	Mu	Ph	Pa	Ma	Dol
CM5	–	–	++	–	–	–	–	–	–	–	–	+	–	–	–
CM6	+	–	+++	+++	–	–	–	–	–	–	+++	+	–	–	+
CM7	–	–	++	++	–	–	–	–	–	–	–	–	–	+	+
CM8	–	–	++	–	–	–	–	–	–	–	–	–	–	–	+
CM9	–	–	+++	+++	+	–	–	–	+	–	–	+	–	–	+++
CM10	–	–	+++	++	–	++	–	–	–	–	–	–	–	–	+++
CM11	+	–	+++	+++	+	–	–	+	–	–	–	+	–	–	+
CM12	–	–	+++	+	–	–	+	–	–	–	–	–	–	–	+++
CM13	++	+	+	+++	–	–	–	–	+	–	+++	–	–	–	–
CM14	–	–	+++	++	–	–	–	++	+	–	–	–	–	–	–
CM15	–	–	+	+++	–	+	–	+++	+	–	–	–	–	–	–
CM16	–	–	+++	++	–	–	+	++	++	–	++	–	–	–	+++
CM17	–	–	+++	+	–	–	–	–	–	++	+	–	+++	–	++
CM18	++	+	+	++	–	–	–	++	+	–	+++	–	–	–	–
CM19	–	–	+++	+	–	+	–	+	–	–	++	++	–	–	++
CM20	–	+++	++	+++	–	–	–	+	+	–	+++	+	–	–	++
CM21	+	–	+++	+++	–	–	–	+	–	–	+	++	+	–	++
CM22	–	–	++	+++	–	+	–	+	–	–	–	+++	–	+	–
CM23	–	–	++	+	–	–	–	–	–	–	–	–	–	–	–
CM24	–	–	++	+++	–	–	–	–	–	–	+	++	–	++	++
CM25	–	–	+	–	–	–	–	–	–	–	+	+	–	–	++
CM26	++	–	+++	+	+	–	–	+	–	–	–	+	++	–	+++
CM27	–	–	+++	+	–	–	+	+	+	–	++	–	–	–	–
CM28	–	–	–	–	–	–	–	–	–	–	–	–	–	–	–

features, and accessory minerals analysis, Proconnesos-1 remains again the most probable source, although some uncertainty remains due to the lack of isotopic data. The isotopic signature of sample CM12 is consistent with Proconnesos-1, Paros Marathi *non-lychnites*, and Aphrodisias-1. The high amounts of dolomite found in the sample allow exclusion of a Parian origin, while the presence of fluorite would seem to support an Anatolian provenance. However, the microstructure and fabric of the sample differ significantly from those typical of both Proconnesos and Aphrodisias marbles. It may in fact represent, albeit with some degree of uncertainty, a fine-grained Proconnesian variety, occasionally quarried and mainly originating from the western sector of the site, as documented in the literature (Beltrame et al., 2019; Attanasio et al., 2008).

- Sample CM10 is a marble with an MGS of 2.16 mm, characteristic of several districts, including Aphrodisias, Proconnesos, Paros Marathi (*lychnites* e *non-lychnites*) and Thasos Vathy–Saliara. However, isotopic data plotted within the reference diagram of the most widely employed ancient Mediterranean fine-grained white marbles indicate a Parian *lychnites* origin. Nonetheless, mineralogical evidence seems to contradict this attribution, given the high dolomite content observed in the sample, which is absent in *lychnites* marbles. Its provenance should therefore be investigated among other minor white marbles. Indeed, this sample appears to exhibit textural characteristics, mineralogical composition, MGS values, and isotopic signature consistent with Ephesos-1 (Kentli Çiftliği, Ahmetli Köyü, Hasançavuşla, Aya Klikiri, and Torbali quarries) (Fig. 10) (Prochaska, 2023; Antonelli and Lazzarini, 2015). However, caution is required in assigning this sample to the Ephesos quarry, since the historical distribution of this marble variety throughout the Empire remains poorly documented, with limited exportation evidence in the literature, and its use was generally reserved for statuary.
- Samples CM13, CM15, CM16, CM17, CM18, and CM27 are fine-grained marbles. In particular, the MGS values indicate that the most plausible sources for samples CM13 and CM17 include Aphrodisias, Docimium, and Paros Marathi (both *lychnites* and *non-lychnites*); for CM18 and CM27, Docimium, Pentelicon and Paros Marathi *lychnites*; for CM15 also Paros Marathi *non-lychnites*; and for CM16, Carrara, Göktepe, Docimium, Pentelicon and Hymettos. Isotopic measurements were key in revealing the provenance of sample CM27, which falls exclusively within the Docimium domain, an affinity also demonstrated by its textural characteristics and mineralogical assemblage (Antonelli et al., 2025). The combination of MGS and isotopic data indicates that samples CM15, CM17, and CM18 are also most likely Docimian marbles. For CM16, the isotopic data restrict the possible provenance to either Docimium or Göktepe; however, the latter can be ruled out due to the extremely pure nature of Göktepe marble, which lacks accessory phases, including dolomite, and exhibits very fine grain size (generally < 0.5 mm) (Prochaska and Attanasio, 2022; Wielgosz-Rondolino et al., 2020; Prochaska et al., 2018; Antonelli and Lazzarini, 2015; Attanasio et al., 2015). For sample CM13, the integration of isotopic results and MGS values suggests affinity with Docimium and Paros Marathi *lychnites*. Although the sample shows a purely calcitic composition, the grey-veined coloration and textural features diverge markedly from those of Parian *lychnites*, which is recognized for its uniformly white colour and absence of trace minerals under petrographic examination, whereas such phases were observed in CM13. For these reasons, CM13 can also be identified as Docimian marble.
- Sample CM23 is likewise a fine-grained marble. Its MGS value falls within the box ranges of Carrara, Göktepe, Docimium and Pentelicon, while isotopic composition confines provenance to the Carrara and Docimium fields. Considering its textural characteristics and polygonal microstructure, with predominantly straight grain boundaries forming triple-junctions, a Carrara origin is the most probable.
- Sample CM20 is also fine-grained, with MGS values consistent with Pentelicon, Docimium and Paros Marathi *lychnites*. Isotopic data allowed exclusion of Docimium and Paros Marathi *lychnites*, since the values fall exclusively within the lower slope of Marble Unit 3 of the Pentelicon quarry. The characteristic schistosity, together with the textural features and abundant occurrence of quartz and micas, already visible under the petrographic microscope, strongly supports this attribution.
- Sample CM28 is a coarse-grained marble. In this case, MGS proved decisive, being diagnostic of the Naxos area, a result also confirmed by isotopic analysis. Indeed, the purely calcitic composition, heteroblastic fabric, mosaic microstructure with strained crystals, and

Table 6
List of the most probable provenance of the white marble samples and final assignment according to the adopted analytical workflow. Legend: Aphr = Aphrodisias; Aphr-1 = Aphrodisias-1; Proc = Proconnesos; Proc-1 = Proconnesos-1; Proc-2 = Proconnesos-2; Nax = Naxos; Par Mar = Paros Marathi; Par Chor = Paros Chorodaki; Thas Al/Ph = Thasos Aliki/Phanari; Thasos Vat/Sal = Thasos Vathy/Saliara; Thas Al = Thasos Aliki; Thasos Acr/Ph = Thasos Acropolis/Phanari; Doc = Docimium; Carr = Carrara; Hym = Hymettos; Gök = Göktepe; Pent = Penteli,

Sample ID	Quarry Matches (MGS)	Quarry Matches (mineralogy/ petrography)	Quarry Matches (isotopes)	Quarry Matches (accessory minerals)	Assignment
CM5	Aphr, Proc, Nax, Par Chor, Thas Al/Ph	Proc	Proc-1, Thas Al	Proc, Thas	Proconnesos-1 (Saraylar)
CM6	Aphr, Proc, Nax, Par Mar, Par Chor, Thas Al/Ph, Thas Vat/Sal	Proc	–	Proc, Thas	Proconnesos-1 (Saraylar)
CM7	Aphr, Proc, Nax, Par Mar, Par Chor, Thas Al/Ph, Thas Vat/Sal	Proc	Pro-1	Proc	Proconnesos-1 (Saraylar)
CM8	Aphr, Proc, Nax, Par Mar, Par Chor, Thas Al/Ph, Thas Vat/Sal	Proc	Proc-1, Thas Al	Not diagnostic	Proconnesos-1 (Saraylar)
CM9	Aphr, Proc, Nax, Par Mar, Par Chor, Thas Al/Ph, Thas Vat/Sal	Proc	Proc-1, Par Mar *non-lychnites*, Thas Al, Thas Acr/Ph	Proc	Proconnesos-1 (Saraylar)
CM10	Aphr, Proc, Nax, Par Mar, Par Chor, Thas Al/Ph, Thas Vat/Sal Eph-1	Eph-1	Par Mar *lychnites,* Eph-1	Not diagnostic	Ephesos-1 (Kentli Çiftliği, Ahmetli Köyü, Hasançavuşla, Aya Klikiri, and Torbali)
CM11	Aphr, Doc, Proc, Pent, Par Mar, Par Chor, Thas Al/Ph, Thas Vat/ Sal	Proc	Proc-1, Thas Al	Proc, Thas	Proconnesos-1 (Saraylar)
CM12	Aphr, Doc, Proc, Nax, Par Mar, Par Chor, Thas Al/Ph, Thas Vat/ Sal	Proc	Proc-1, Par Mar *non-lychnites*, Aphr-1	Proc, Aphr	Proconnesos-1 (Saraylar)
CM13	Carr, Aphr, Doc, Gök, Proc, Pent, Par Mar, Par Chor, Thas Vat/Sal	Doc	Doc, Gök, Par Mar *lychnites*	Doc	Docimium
CM14	Aphr, Doc, Proc, Nax, Par Mar, Par Chor, Thas Al/Ph, Thas Vat/ Sal	Proc	Proc-1, Thas Al	Proc	Proconnesos-1 (Saraylar)
CM15	Carr, Aphr, Doc, Gök, Proc, Pent, Par Mar, Par Chor, Thas Vat/Sal	Doc	Doc, Gök	Doc	Docimium
CM16	Carr, Aphr, Doc, Gök, Proc, Pent, Hym, Par Mar, Par Chor	Doc	Doc, Gök	Doc	Docimium
CM17	Carr, Aphr, Doc, Gök, Proc, Pent, Par Mar, Par Chor, Thas Vat/Sal	Doc	Pent, Doc	Doc	Docimium
CM18	Carr, Aphr, Doc, Gök, Proc, Pent, Hym, Par Mar, Par Chor, Thas Vat/Sal	Doc	Doc, Gök	Doc	Docimium
CM19	Aphr, Proc, Nax, Par Mar, Par Chor, Thas Al/Ph, Thas Vat/Sal	Proc	Proc-2, Thas Vat/Sal	Proc	Proconnesos-2 (Camlik)
CM20	Carr, Aphr, Doc, Gök, Proc, Pent, Par Mar, Par Chor, Thas Vat/Sal	Pent	Pent	Pent	Penteli
CM21	Aphr, Proc, Nax, Par Mar, Par Chor, Thas Al/Ph, Thas Vat/Sal	Proc	Proc-1, Par Mar *non-lychnites*, Thas Al	Proc	Proconnesos-1 (Saraylar)
CM22	Aphr, Doc, Proc, Nax, Par Mar, Par Chor, Thas Al/Ph, Thas Vat/ Sal	Proc	Proc-1, Thas Al	Proc	Proconnesos-1 (Saraylar)
CM23	Carr, Aphr, Doc, Gök, Proc, Pent, Hym, Par Mar, Par Chor, Thas Vat/Sal	Carr	Carr, Hym, Doc	Carr	Carrara
CM24	Aphr, Doc, Gök, Proc, Pent, Par Mar, Paros Chor, Thasos Vat/Sal	Proc	Proc-1, Par Mar *non-lychnites*, Aphr-1	Proc	Proconnesos-1 (Saraylar)
CM25	Aphr, Proc, Nax, Par Mar, Par Chor, Thas Al/Ph, Thas Vat/Sal	Proc	Proc-1, Thas Al	Proc, Thas	Proconnesos-1 (Saraylar)
CM26	Aphr, Proc, Nax, Par Mar, Par Chor, Thas Al/Ph, Thas Vat/Sal	Proc	Procs-1, Par Mar *non-lychnites*, Thas Al, Par Chor, Thas Acr/ Ph	Proc	Proconnesos-1 (Saraylar)
CM27	Carr, Aphr, Doc, Gök, Proc, Pent, Par Mar, Par Chor, Thas Vat/Sal	Doc	Doc	Doc	Docimium
CM28	Nax, Thas Al/Ph	Nax	Nax, Aphr, Thas Acr/Ph	Nax	Naxos

predominantly sutured to embayed grain-boundary shapes are typical of Naxian marble.

As a result of the analysis, the most-likely geographical provenance of the white-marble *tesserae* from the "*A Grandi Fiori*" mosaic of the Roman Villa of Casignana are provided in Table 7.

Thus, the archaeometric investigation reveals that the mosaic is not composed of a single marble type from a unique source. Instead, it results from the juxtaposition of *tesserae* obtained from marble blocks quarried in different regions of the Empire, particularly Asia Minor and, to a lesser extent, Greece and Italy. This finding is significant and opens new perspectives on the criteria adopted by the workshop in selecting raw materials.

The results achieved suggest the predominant role of the Proconnesian quarries as the main supply source for the mosaic studied. This is fully consistent with the widespread popularity of the marbles of the island of Marmara in Italy and the Eastern Mediterranean during the Middle and Late Empire, which is precisely the period when the "*A Grandi Fiori*" mosaic was executed. Indeed, in this phase, Proconnesian marble ultimately displaced Carrara marble in public architecture (Taelman, 2022; Al-Bashaireh, 2021; Pensabene, 2013; Attanasio et al., 2008).

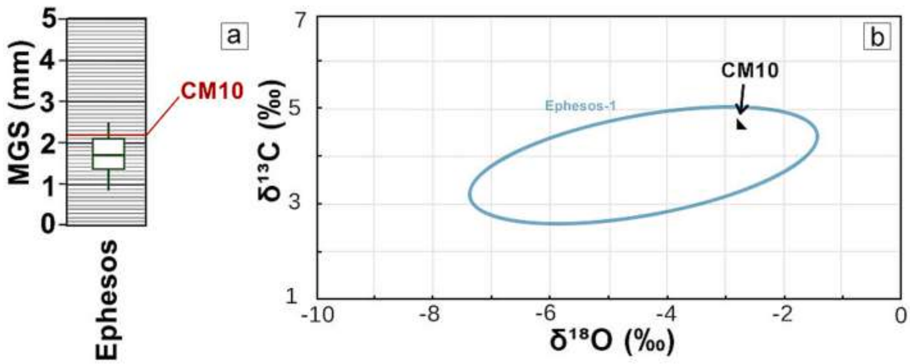

Fig. 10. MGS and stable isotopic values of sample CM10 plotted on (a) the reference maximum MGS box bar and (b) the isotopic reference field of Ephesian white marble respectively from Antonelli and Lazzarini (2015) and Prochaska (2023).

Table 7
Hypothesised provenance and relative occurrence of white marble *tesserae* by provenance field, expressed as their percentage of the total analyzed *tesserae*.

Hypothesised provenance	Sample ID		Relative occurrence
Proconnesos-1 (Saraylar)	CM5	CM14	58.33%
	CM6	CM21	
	CM7	CM22	
	CM8	CM24	
	CM9	CM25	
	CM11	CM26	
	CM12		
Proconnesos-2 (Camlik)	CM19		
Docimium	CM13	CM17	25.00%
	CM15	CM18	
	CM16	CM27	
Pentelicon	CM20		4.16%
Carrara	CM23		4.16%
Naxos	CM28		4.16%
Ephesos-1 (Kentli Çiftliği, Ahmetli Köyü, Hasançavuşla, Aya Klikiri, and Torbali)	CM10		4.16%

The diffusion of Proconnesian marble in Italy during the Severan period (late 2nd–early 3rd century CE) is further confirmed by the stone cargoes documented in Roman shipwrecks. Proconnesian blocks were found in southern Italy, for example, on the Punta Scifo wreck (200–250 CE), located south of Crotone and not far from Casignana, as well as in the wrecks of Isola delle Correnti, Capo Granitola and Marzamemi in Sicily (all 3rd century CE) (Beltrame et al., 2019; Beltrame et al., 2016). Indeed, the 3rd century witnessed an intensification of maritime transport between Italy and the East, driven by extensive building and restoration programmes promoted by the Severan emperors (Antonelli et al., 2020). The success of Proconnesian marble may be attributed to several factors, including the strategic and easily accessible location of the quarries on the northern coast of the island of Marmara, the availability of a highly specialised workforce, and an efficient production and export system, all of which contributed to significantly reducing material costs. As a result, Eastern marbles, and particularly Proconnesian, are systematically attested in many Late Imperial sites.

The relative frequency of the marble varieties used in the "*A Grandi Fiori*" mosaic broadly reflects the statistical distribution documented for architectural marble artefacts in Italy during the same period: Pentelic, Carrara, Docimium and, to a lesser extent, Naxian marble occur as the most common varieties after the widely diffused Proconnesian type (Taelman, 2022). Ephesian marble intended for architectural use is not attested in Italy, although the variety is well documented in the Eastern Mediterranean.

However, given the low frequency of the Docimium, Pentelic, Carrara, Naxian and Ephesian *tesserae*, the possibility of recycling and reusing marble elements cannot be excluded. Reuse became a widespread practice in Late Antiquity, when large quantities of marble from earlier decorative elements or abandoned structures were reworked and adapted to new contexts.

Significantly, the Villa underwent extensive renovation and expansion during the 3rd century, contemporaneous with the creation of the "*A Grandi Fiori*" mosaic. These works included the introduction of heated rooms in the seaside residential complex, the doubling of the bathing circuit in the upland complex, and the installation of the first-floor mosaics composed of large white, black and green *tesserae* in Rooms 9, 15, M, O, Q and also Room N. In this context, it is plausible that materials derived from the transformation of earlier spaces were at least partially reworked and incorporated into the new monumental decorative programme commissioned by the villa's owner.

Overall, the selection of quarries other than Proconnesus for the "*A Grandi Fiori*" mosaic seems primarily linked to economic considerations and material availability, whether already on site or derived from reused elements. There appear to be no aesthetic reasons or specific design requirements that would necessitate the inclusion of additional marble types. Proconnesian marble already offers a broad range of tones, from white to greyish, more than adequate to meet the chromatic needs of the mosaic and is also considered the most economical of the white marbles available on the market during the 3rd century (Giacchero, 1974).

Further archaeometric studies on additional architectural elements from the villa, including those belonging to its different chronological phases, will be essential to clarify this aspect.

5. Conclusions

The archaeometric study conducted on the green and white *tesserae* composing the "*A Grandi Fiori*" mosaic in "Room N" of the residential area of the Roman Villa at Palazzi di Casignana provided important information about the characterization and the provenance of the raw materials, adding new elements to the archaeological context of the villa.

The green *tesserae* are biomicrite/mudstone limestones containing microfossils embedded in a micritic matrix. XRD confirms their predominantly calcitic composition with minor quartz, clay minerals and whewellite, while SEM-EDS identifies high iron amounts throughout the matrix, likely responsible for the green coloration. The mineropetrographic features of the green *tesserae* suggest a probable local provenance from the Cretaceous-Lower Miocene Variegated Clays Formation around Casignana. Further studies, including microfossil comparison with local outcrops, will confirm this hypothesis.

Petrographic and geochemical analyses of the white *tesserae* indicate the use of marbles sourced from various regions of the Roman Empire, including Asia Minor, Greece and Italy, with a clear predominance of Proconnesian marble. This finding aligns with known patterns of lithotype circulation and exploitation in the 3rd century CE, when the marble from the island of Marmara was economically competitive and readily available due to an organized extraction and export system, making it the primary source for architectural elements.

The limited presence of other Anatolian, Greek and Italian marbles (Docimium, Pentelicon, Naxian, Carrara, and possibly Ephesos) does not appear to reflect aesthetic considerations or specific design choices. Instead, it is more likely that these materials were used because they were more readily available or reused, a common practice in Late Antiquity. This hypothesis is supported by the extensive renovations and modifications carried out in the villa during that period.

Overall, the results achieved in this work highlight the *modus operandi* of past craftsmen, who combined materials likely of local provenance with valuable ones (i.e. white marbles) from various Mediterranean regions. This provides important archaeological implications regarding the status of the villa's owners, the marbles trade routes, and stylistic trends of the historical period.

Funding sources

This research is funded by PNRR, TECH4YOU – "Technologies for Climate Change Adaptation and Quality of Life Improvement", CUP H23C22000370006, Project Code: ECS_00000009.

CRediT authorship contribution statement

Maria Antonietta Zicarelli: Writing – review & editing, Writing – original draft, Methodology, Investigation, Formal analysis, Data curation. **Luciana Randazzo:** Writing – review & editing, Writing – original draft, Methodology, Investigation, Formal analysis, Data curation. **Natalia Rovella:** Writing – review & editing, Writing – original draft, Data curation. **Donatella Barca:** Conceptualization. **Mauro Francesco La Russa:** Supervision, Conceptualization. **Michela Ricca:** Writing – review & editing, Writing – original draft, Supervision, Methodology, Investigation, Formal analysis, Data curation, Conceptualization.

Declaration of competing interest

The authors declare that they have no known competing financial interests or personal relationships that could have appeared to influence the work reported in this paper.

Acknowledgments

This research was carried out with the support of the PNRR under the project TECH4YOU – Technologies for Climate Change Adaptation and Quality of Life Improvement, whose contribution is gratefully acknowledged. The authors sincerely thank Professor Giovanna Scopelliti for her valuable assistance with the isotopic analyses. They also wish to express their appreciation to the two anonymous reviewers for their insightful comments and constructive suggestions, which substantially improved the quality and clarity of the manuscript.

Data availability

Data will be made available on request.

References

Al-Bashaireh, K., 2021. Ancient white marble trade and its provenance determination. J. Archaeol. Sci. Rep. 35, 102777. https://doi.org/10.1016/j.jasrep.2020.102777.

Antonelli, F., Lazzarini, L., 2015. An updated petrographic and isotopic reference database for white marbles used in Antiquity. Rend. Fis. Acc. Lincei 26, 399–413. https://doi.org/10.1007/s12210-015-0423-4.

Antonelli, F., Bloise, A., Bruno, F., De Luca, R., Allegretta, I., Medaglia, S., Grasso, A.T., Terzano, R., Miriello, D., 2020. Archaeometric approach to identifying the provenance of white marbles from the shipwreck of Cala Cicala (Crotone, Calabria, Italy). J. Arch. Sci. R 30, 102204. https://doi.org/10.1016/j.jasrep.2020.102204.

Antonelli, F., Poggio, A., Cancelliere, S., 2025. Marmora Vesuviana: archaeometric analyses of marble artifacts in the Granai del Foro in Pompeii. Rend. Fis. Acc. Lincei 36, 7–22. https://doi.org/10.1007/s12210-025-01315-7.

Attanasio, D., Brilli, M., Bruno, M., 2008. The properties and identification of marble from Proconnesos (Marmara Island, Turkey): a new database including isotopic, EPR and petrographic data. Archaeometry 50 (5). https://doi.org/10.1111/j.1475-4754.2007.00364.x.

Attanasio, D., Brilli, M., Ogle, N., 2006. The isotopic signatures of classical marbles. L'erma di Bretschneider, Rome 279. [Google Scholar].

Attanasio, D., Bruno, M., Prochaska, W., Yavuz, A.B., 2015. A multi method database of the black and white marbles of Göktepe (Aphrodisias), including isotopic, EPR, trace and petrographic data. Archaeometry 57(2), 217–245. https://doi.org/10. 1111/arcm.12076.

Barca, D., Fiorenza, E., D'Andrea, M., Le Pera, E., Musella, M., Sudano, F., Taliano Grasso, A., 2019. Chemical and Petrographic Characterization of Stone and Glass Tesserae in the Nereid and Geometric Mosaics from the S. Aloe Quarter in Vibo Valentia–Calabria, Italy. Minerals 9, 729. https://doi.org/10.3390/min9120729.

Beltrame, C., Lazzarini, L., Parizzi, S., 2016. The Roman ship 'Punta Scifo D'and its marble cargo (Crotone, Italy). Oxf. J. Archaeol. 35 (3), 295–326. https://doi.org/10.1111/ojoa.12091.

Beltrame, C., Percic, T., Lazzarini, L., 2019. The archaeometric identification of the marbles of the Roman shipwrecks of Capo Granitola (TP), Isola Delle Correnti and Marzamemi I (SR). J. Archaeol. Sci. Rep. 23, 953–967. https://doi.org/10.1016/j.jasrep.2018.11.021.

Bruni, M., 2009. The Monumental Villa at Palazzi di Casignana and the Roman Elite in Calabria (Italy) during the Fourth Century AD, PhD Dissertation, University of California, Berkeley, United States. https://escholarship.org/uc/item/2jf6g36f.

Capedri, S., Venturelli, G., 2004. ACCESSORY MINERALS AS TRACERS IN THE PROVENANCING OF ARCHAEOLOGICAL MARBLES, USED IN COMBINATION WITH ISOTOPIC AND PETROGRAPHIC DATA. Archaeometry 46, 517–536. https://doi.org/10.1111/j.1475-4754.2004.00171.x.

Capedri, S., Venturelli, G., Photiades, A., 2004. Accessory minerals and δ18O and δ13C of marbles from the Mediterranean area. J. Cult. Herit. 5 (1), 27–47. https://doi.org/10.1016/j.culher.2003.03.003.

Cavazza, W., Barone, M., 2010. Large-scale sedimentary recycling of tectonic mélange in a forearc setting: the Ionian basin (Oligocene–Quaternary, southern Italy). Geol. Soc. Am. Bull. 122 (11–12), 1932–1949. https://doi.org/10.1130/B30177.1.

Critelli, S., Muto, F., Tripodi, V., 2016. Note illustrative della Carta Geologica D'Italia alla scala 1: 50.000 foglio 603 Bovalino. ISPRA (Istituto Superiore per la Protezione e la Ricerca Ambientale). Servizio Geologico D'italia, Progetto CARG. https://www.isprambiente.gov.it/Media/carg/note_illustrative/603_Bovalino.pdf.

Dunham, R.J., 1962. Classification of carbonate rocks according to depositional texture. In: Ham, W.E. (Ed.), Classification of Carbon Ate Rocks. AAPG, Tulsa. [Google Scholar], pp. 108–121.

Flügel, E., Flügel, C., 1997. Applied microfacies analysis: Provenance studies of Roman mosaic stones. Facies 37, 1–48. https://doi.org/10.1007/BF02537369.

Folk, R.L., 1962. Spectral subdivision on limestone types, in: Ham, W.E. (Ed.), Classification of carbonate rocks. AAPG, Tulsa, pp. 62–84 [Google Scholar].

Giacchero, M., 1974. Edictum Diocletiani et Collegarum de pretiis rerum venalium. Istituto di storia antica e scienze ausiliarie, Genova. [Google Scholar].

Gorgoni, C., Lazzarini, L., Pallante, P., Turi, B., 2002. In: An Updated and Detailed Mineropetrographic and CO Stable Isotopic Reference Database for the Main Mediterranean Marbles Used in Antiquity. [Google Scholar], pp. 115–131.

Grillo, E., 2014. Il Mosaico Con Il 'trionfo Indiano Di Dioniso' Dalla Villa Romana Di Palazzi Di Casignana (RC). Scripta Manent, Tivoli.

Lazzarini, L., Moschini, G., Stievano, B.M., 1980. A contribution to the identification of italian, Greek and Anatolian marbles through a petro-logical study and the evaluation of calcium/strontium ratio. Archaeometry 22 (2), 173–183. https://doi.org/10.1111/j.1475-4754.1980.tb00940.x.

Malacrino, C. G., 2014. I nuclei termali delle ville romane calabresi fra il II e il IV secolo d.C.: Roggiano Gravina, Malvito e Casignana, in: Pensabene, P., Sfameni, C. (Eds.), La villa restaurata e i nuovi studi sull'edilizia residenziale tardoantica. Edipuglia, Bari. [Google Scholar].

Maniatis, Y., Damaskos, D., Prochaska, W., Anevlavi, V., Tambakopoulos, D., 2024. Scientific investigation on the provenance of marble of free-standing sculptures from the archaeological museum of Kavala/northern Greece. Archaeol. Anthropol. Sci. 16, 125. https://doi.org/10.1007/s12520-024-02028-y.

Moens, L., Roos, P., De Rudder, J., De Paepe, P., Van Hende, J., Marechal, R., Waelkens, M., 1988. A multi-method approach to the identification of white marbles used in antique artifacts. In: Herz, N., Waelkens, M. (Eds.), Classical Marble: Geochemistry, Technology, Trade. Kluwer Academic Publishers, Dordrecht, pp. 243–250. https://doi.org/10.1007/978-94-015-7795-3_27.

Munro, B., 2011. Approaching architectural recycling in roman and late roman villas, in: Mladenivic, D., Russel, B. (Eds.), Proceedings of the Twentieth Annual Theoretical Roman Archaeology Conference, Oxford, pp. 76–88. [Google Scholar].

Musso, L., Buccino, L., Bruno, M., Attanasio, D., Prochaska, W. 2018. Marble and sculpture at Lepcis Magna (Tripolitania, Libya): a preliminary study concerning origin and workshops, in: Poljak, D.M., Marasović, K., (Eds.), ASMOSIA 11: Interdisciplinary studies on ancient stone—Proceedings of the Eleventh International Conference of the Association for the Study of Marble and Other Stones in Antiquity. Split, pp. 481–490. https://doi.org/10.31534/XI.asmosia.2015/02.32.

Pensabene, P., 2013. I marmi nella Roma antica. Carocci, Rome. [Google Scholar].

Pike, S., 2025. Characterization of Intra-Quarry Variability in Pentelic Marble using Stable Isotopes: a Case Study of the Parthenon. Minerals 15, 231. https://doi.org/10.3390/min15030231.

Prochaska, W., 2023. The use of geochemical methods to pinpoint the origin of ancient white marbles. Miner. Petrol. 117, 401–409. https://doi.org/10.1007/s00710-023-00833-2.

Prochaska, W., Attanasio, D., 2022. The challenge of a successful discrimination of ancient marbles (part III): a databank for Aphrodisias, Carrara, Dokimeion, Göktepe, Hymettos, Parian Lychnites and Pentelikon. J. Archaeol. Sci. Rep. 45, 103582. https://doi.org/10.1016/j.jasrep.2022.103582.

Prochaska, W., Attanasio, D., Bruno, M., 2018. Unraveling the Carrara Göktepe entanglement, in: Matetíc Poljak, D., Marasovíc, K. (Eds.), ASMOSIA XI. Interdisciplinary Studies of Ancient Stone. Proceedings of the Eleventh International Conference of ASMOSIA, Split, 18–22 May 2015. Arts Academy in Split – University of Split, University of Split – Faculty of Civil Engineering, Archi tecture and Geodesy, Split, pp. 175–183. [Google Scholar].

Prochaska, W., Attanasio, D., 2021. The challenge of a successful discrimination of ancient marbles (part I): a databank for the marbles from Paros, Prokonnesos, Heraklea/Miletos and Thasos. J. Archaeol. Sci. Rep. 35, 102676. https://doi.org/10.1016/j.jasrep.2020.102676.

Rampazzi, L., 2019. Calcium oxalate films on works of art: a review. J. Cult. Herit. 40, 195–214. https://doi.org/10.1016/j.culher.2019.03.002.

Ricca, M., Belfiore, C.M., Ruffolo, S.A., Barca, D., De Buergo, M.A., Crisci, G.M., La Russa, M.F., 2015. Multi-analytical approach applied to the provenance study of marbles used as covering slabs in the archaeological submerged site of Baia (Naples, Italy): the case of the "Villa con ingresso a protiro". Appl. Surf. Sci. 357, 1369–1379. https://doi.org/10.1016/j.apsusc.2015.10.002.

Ricca, M., Urzì, C.E., Rovella, N., Sardella, A., Bonazza, A., Ruffolo, S.A., De Leo, F., Randazzo, L., Arcudi, A., La Russa, M.F., 2020. Multidisciplinary approach to characterize archaeological materials and status of conservation of the roman Thermae of Reggio Calabria site (Calabria, south Italy). Appl. Sci. 10 (15), 5106. https://doi.org/10.3390/app10155106.

Rovella, N., Musella, M., Barca, D., 2022. Characterization of stone tesserae from "The Indian Triumph of Dionysus" Mosaic (Casignana, Reggio Calabria, Italy). J. Phys.: Conf. Ser. 2204(1), 012036. https://doi.org/10.1088/1742-6596/2204/1/012036.

Sabbione, C., 2007. La villa romana di Palazzi di Casignana, guida archeologica. Corab, Gioiosa Jonica. [google Scholar].

Sabbione, C., Barello, F., Brizzi, M., Cardosa, M., 1997. I mosaici dell'edificio termale in contrada palazzi di Casignana (Reggio Calabria), in: VV.AA. (Eds.), Proceedings of the IV Colloquio dell'Associazione Italiana per lo Studio e la Conservazione del Mosaico, Palermo, 9-13 Dicembre 1996. Edizioni del Girasole, Ravenna, pp. 385-400.

Stern, H., 1975. La Funzione del mosaico nella casa antica. In: Mirabella Roberti, M. (Ed.), Mosaici in Aquileia e Nell'alto Adriatico. Arti Grafiche Friulana, Udine, pp. 39–57.

Taelman, D., 2022. Marble Trade in the Roman Mediterranean: a Quantitative and Diachronic Study. J. Rom. Archaeol. 35, 848–875. https://doi.org/10.1017/S1047759422000447.

Wielgosz-Rondolino, D., Antonelli, F., Bojanowski, M.J., Gładki, M., Göncüoğlu, M.C., Lazzarini, L., 2020. Improved methodology for identification of Göktepe white marble and the understand ing of its use: a comparison with Carrara marble. J. Archaeol. Sci. 113, 105059. https://doi.org/10.1016/j. jas. 2019.105059.

Further reading

Prochaska, W., Ladstätter, S., Anevlavi, V., 2023. The challenge of a successful discrimination of ancient marbles (part IV): a databank for the white marbles from the region of Ephesos. J. Archaeol. Sci. Rep. 53, 104336. https://doi.org/10.1016/j.jasrep.2023.104336.